Trajectories of trojan bodies

Author: Gerhard Kirchner

Abstract

As a well known fact, Jupiter can trap asteroids or other bodies near the Lagrange points L_4 and L_5 which form equilateral triangles with the base line Sun-Jupiter (generally Sun-Planet). My intention is to analyze trajectories of bodies moving in the neighborhood of L4. I refer to the article https://wmap.gsfc.nasa.gov./media/ContentMedia/lagrange.pdf where Neil J. Cornish derives the linearized equation of motion in a corotating system with L_4 as origin.
I will derive the solution to this equation which leads to a superposition of two periodic motions. One period T_2 is close to the orbit period T_p of the planet, T_1 is considerably greater. In the 3-dimensional case, there is an additional oscillation with the period T_p (see annotation at the end of ch. II).
A good approximation of the general solution can be obtained by a tailor series which reveals four basic components of the movement.
The solution to the linearized equation of motion is valid only for small velocities and small distances from L_4. A numeric iteration will show the limits of linearity. With a moderate number of iteration steps, good results are found. As to elliptic planet orbits, the modifications are small. However, the trajectory of a body in the Sun-Earth system is perturbed by Jupiter such that no trojan can be trapped closer to L_4 than about 10^6 km over a long time.

page

Contents

I Linearized equation of motion (referring to the article cited above)

$$\frac{d}{dt}\begin{pmatrix}\delta x\\ \delta y\\ \delta v_x\\ \delta v_y\end{pmatrix}=\begin{pmatrix}0 & 0 & 1 & 0\\ 0 & 0 & 0 & 1\\ 3\Omega^2/4 & 3\sqrt{3}\kappa\Omega^2/4 & 0 & 2\Omega\\ 3\sqrt{3}\kappa\Omega^2/4 & 9\Omega^2/4 & -2\Omega & 0\end{pmatrix}\begin{pmatrix}\delta x\\ \delta y\\ \delta v_x\\ \delta v_y\end{pmatrix}\qquad (1.16)\text{ and }(1.22),$$

where δx and δy are the coordinates referring to L_4 as origin and a frame corotating with the Sun-Planet system (angular velocity Ω) and δv_x, δv_y the corresponding velocity components in this system. $\kappa=\frac{M_1-M_2}{M_1+M_2}$ is a mass ratio with the sun mass M_1 and the planet mass M_2.

The eigenvalues of the matrix are

$$\lambda_\pm=\pm i\frac{\Omega}{2}\sqrt{2-\sqrt{27\kappa^2-23}},\qquad \sigma_\pm=\pm i\frac{\Omega}{2}\sqrt{2+\sqrt{27\kappa^2-23}}\qquad (1.23)$$

II Derivation of the solution

For simplicity, "δ" will be omitted. This means that the origin of the coordinate system now is the Lagrange point (and not the barycenter).

Equation of motion (notation $\dot{x}=\frac{dx}{dt}$ etc.):

$$\begin{pmatrix}\dot{x}\\ \dot{y}\\ \ddot{x}\\ \ddot{y}\end{pmatrix}=A(\Omega)\cdot\begin{pmatrix}x\\ y\\ \dot{x}\\ \dot{y}\end{pmatrix}\text{ with } A(\Omega)=\frac{1}{4}\begin{pmatrix}0 & 0 & 4 & 0\\ 0 & 0 & 0 & 4\\ 3\Omega^2 & \gamma\Omega^2 & 0 & 8\Omega\\ \gamma\Omega^2 & 9\Omega^2 & -8\Omega & 0\end{pmatrix}\text{ and } \gamma=3\sqrt{3}\kappa\qquad (2.1)$$

When λ is an eigenvalue of $A(\Omega)$ and $\vec{h}(\lambda)$ a corresponding eigenvector, (2.1) is solved by $\vec{h}(\lambda)\cdot e^{\lambda t}$ because $\frac{d}{dt}\left(\vec{h}(\lambda)\cdot e^{\lambda t}\right)=\lambda\cdot\left(\vec{h}(\lambda)\cdot e^{\lambda t}\right)=A(\Omega)\cdot\left(\vec{h}(\lambda)\cdot e^{\lambda t}\right)$.

The general solution is a linear combination of such terms. Apart from a constant factor:

$$\vec{h}(\lambda)=(9-4\mu^2,\ 8\mu-\gamma,\ \lambda(9-4\mu^2),\ \lambda(8\mu-\gamma))^T \text{ with } \mu=\lambda/\Omega\qquad (2.2)$$

Proof of (2.2):

$$A(\Omega)\cdot\vec{h}(\lambda)-\lambda\cdot\vec{h}(\lambda)=\tfrac{1}{4}(0,0,F(\mu),0)^T \text{ with } F(\mu)=16\mu^4+16\mu^2-\gamma^2+27$$

$F(\mu)=0$ is solved by $\mu=\pm\frac{i}{2}\sqrt{2\pm\sqrt{\gamma^2-23}}$

In accordance with (1.23); the eigenvalues are:

$$\lambda_1=i\Omega f,\lambda_2=-i\Omega f,\lambda_3=i\Omega g,\lambda_4=-i\Omega g \tag{2.3}$$

with $f=\frac{1}{2}\sqrt{2-\sqrt{\gamma^2-23}}$ and $g=\frac{1}{2}\sqrt{2+\sqrt{\gamma^2-23}}$ $\quad(f^2+g^2=1)$

(2.2) and (2.3) lead to the matrix of eigenvectors:

$$\left(\vec{h}_1,\vec{h}_2,\vec{h}_3,\vec{h}_4\right)=\begin{pmatrix}\alpha & \alpha & \beta & \beta\\ 8if-\gamma & -8if-\gamma & 8ig-\gamma & -8ig-\gamma\\ i\Omega\alpha f & -i\Omega\alpha f & i\Omega\beta g & -i\Omega\beta g\\ -\Omega(8f^2+i\gamma f) & -\Omega(8f^2-i\gamma f) & -\Omega(8g^2+i\gamma g) & -\Omega(8g^2-i\gamma g)\end{pmatrix} \tag{2.4}$$

with $\alpha=9+4f^2$ and $\beta=9+4g^2=13-4f^2$

Split into real and imaginary parts:

$\left(\vec{h}_1,\vec{h}_2,\vec{h}_3,\vec{h}_4\right)=(\vec{u}_1+i\vec{u}_2,\vec{u}_1-i\vec{u}_2,\vec{u}_3+i\vec{u}_4,\vec{u}_3-i\vec{u}_4)$

$$\text{with } M_u=(\vec{u}_1,\vec{u}_2,\vec{u}_3,\vec{u}_4)=\begin{pmatrix}\alpha & 0 & \beta & 0\\ -\gamma & 8f & -\gamma & 8g\\ 0 & \Omega f\alpha & 0 & \Omega g\beta\\ -8\Omega f^2 & -\Omega f\gamma & -8\Omega g^2 & -\Omega g\gamma\end{pmatrix} \tag{2.5}$$

(2.1) is generally solved by $\overrightarrow{W}(t)=\sum_{n=1}^{4}(r_n+is_n)\cdot\vec{h}_n\cdot e^{\lambda_n\cdot t}$, r_n and s_n real.

The imaginary part of $\overrightarrow{W}(t)$ vanishes because the starting vector $\overrightarrow{W}(0)$ is real.

By a straightforward transformation, one obtains

$$\begin{aligned}\overrightarrow{W}(t)=&(c_1\vec{u}_1+c_2\vec{u}_2)\cos(\Omega ft)+(c_2\vec{u}_1-c_1\vec{u}_2)\sin(\Omega ft)\\ &+(c_3\vec{u}_3+c_4\vec{u}_4)\cos(\Omega gt)+(c_4\vec{u}_3-c_3\vec{u}_4)\sin(\Omega gt)\end{aligned} \tag{2.6}$$

with $c_1 = r_1 + r_2,\ c_2 = s_2 - s_1, c_3 = r_3 + r_4$ and $c_4 = s_4 - s_3$.

The coefficients r_n, s_n are obsolete now such that four free parameters c_1, c_2, c_3 and c_4 remain. With (2.6):

$$\vec{W}(0) = (x_0, y_0, \dot{x}_0, \dot{y}_0)^T = c_1\vec{u}_1 + c_2\vec{u}_2 + c_3\vec{u}_3 + c_4\vec{u}_4 = M_u \cdot (c_1, c_2, c_3, c_4)^T \qquad (2.7)$$

is the starting vector which is normally given.

By inversion of M_u, one obtains:

$$\begin{pmatrix} c_1 \\ c_2 \\ c_3 \\ c_4 \end{pmatrix} = \frac{1}{z}\begin{pmatrix} \gamma^2 + 64g^2 & \gamma\beta & 0 & 8\beta \\ 2\gamma\beta/f & 18\beta/f & (\gamma^2 - 144)/f & \gamma\beta/f \\ -(\gamma^2 + 64f^2) & -\alpha\gamma & 0 & -8\alpha \\ -2\alpha\gamma/g & -18\alpha/g & -(\gamma^2 - 144)/g & -\alpha\gamma/g \end{pmatrix}\begin{pmatrix} x_0 \\ y_0 \\ \dot{x}_0/\Omega \\ \dot{y}_0/\Omega \end{pmatrix} \qquad (2.8)$$

with $z = 4(144 - \gamma^2)(1 - 2f^2)$.

$$\vec{q} = (x_0, y_0, \dot{x}_0/\Omega, \dot{y}_0/\Omega)^T \qquad (2.9)$$

modifies the starting vector such that all components have the dimension of a length.

The spatial components of $\vec{W}(t)$ in (2.6) completely describe the movement of the body:

$$\begin{bmatrix} x(t) = c_1\alpha\cos(\Omega ft) + c_2\alpha\, sin(\Omega ft) + c_3\beta\cos(\Omega gt) + c_4\beta\, sin(\Omega gt) \\ y(t) = (8fc_2 - \gamma c_1)\cos(\Omega ft) - (8fc_1 + \gamma c_2)\, sin(\Omega ft) \\ \quad +\ (8gc_4 - \gamma c_3)\cos(\Omega gt) - (8gc_3 + \gamma c_4)\, sin(\Omega gt) \end{bmatrix} \qquad (2.10)$$

Annotation:

Extending the movement in the z-direction (perpendicular to the ecliptic plane), one finds (in the linear approximation): $\ddot{z} = -\frac{GM_1 + GM_2}{R^3} z = -\Omega^2 z$ (Kepler's law).

This leads to a harmonic z-oscillation with the angular frequency Ω.

For $z(0) = 0$: $z(t) = \frac{\dot{z}(0)}{\Omega} sin\ (\Omega t)$

III Examples

Data for the earth ($f = 0.0045, g = 1 - 10^5$) and Jupiter($f = 0.08, g = 1 - 10^3$) :

Orbit period of the planet: $T = \frac{2\pi}{\Omega}$ (Earth: 1a, Jupiter: 11.9a)

Short period of the trojan body: $T_1 = \frac{T}{g} \approx T$

Long period : $T_1 = \frac{T}{f}$ (Earth: 222a, Jupiter: 12.4*11.9a = 147a)

Using the velocity unit $v = 1\frac{m}{s}$ and the length unit $u = 1\frac{m}{s}/\Omega$ (see 2.9):

Earth: $u = 5023\ km$, Jupiter: $u = 59492\ km$

(3.1)

(2.10) is valid only for small distances from L_4 and small velocities. The units u and v can be considered as small in this sense.

The coefficients in (2.10) depend on the position and the velocity vector of the body at an initial time. The description of the trajectory is easier in a (x', y')-system, rotated by 30° vs. the (x, y)-system (fig. III.1b). For simplicity, the body starts on one of the axes with velocity zero or at L_4 with velocity u. The planet is the earth (left figure) or Jupiter (right figure). d_{max} is the maximum distance from L_4.

In case of the earth, the motion of the body mainly is an oscillation along the x'-axis with the long period. The zoom reveals an additional y'-oscillation with a small amplitude such that the tajectory is elliptic. In case of Jupiter, the approximate ellipse can be seen without zoom.

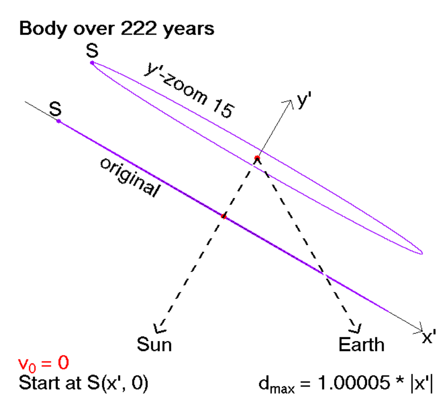

Fig. III.1a

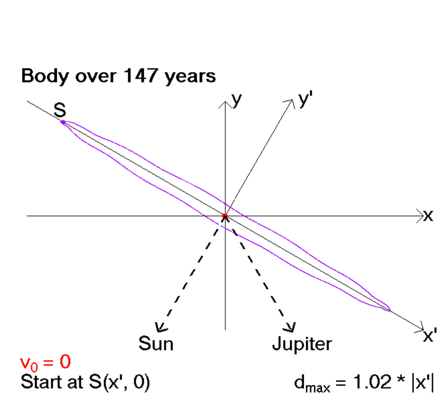

Fig. III.1b

In both cases, the body starts on the y'-axis. It needs a zoom to distinguish S from L_4.
Earth: The y'-zoom shows the oscillations with the small period of one year.
Jupiter: The trajectory is more chaotic, but about 12 loops with the small period of about 12 years can be distinguished.

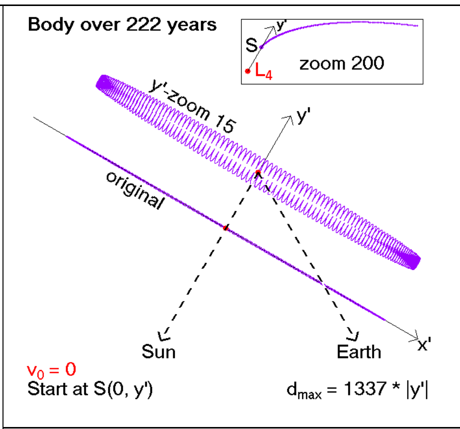

Fig. III.2a

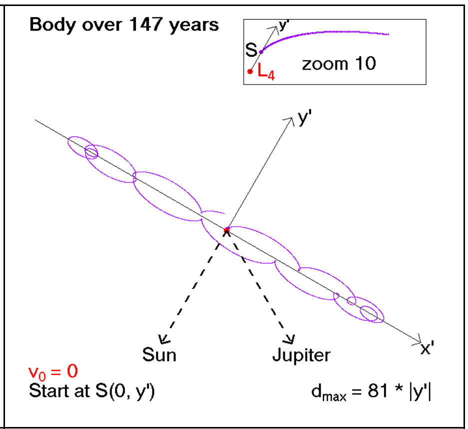

Fig. III.2b

When $\vec{v_0}$ is directed along the x'-axis, the body is deflected by the Coriolis force (see zoom in the rectangle) such that it mainly moves in the opposite direction.
d_{max} is rather great considering the small initial velocity.

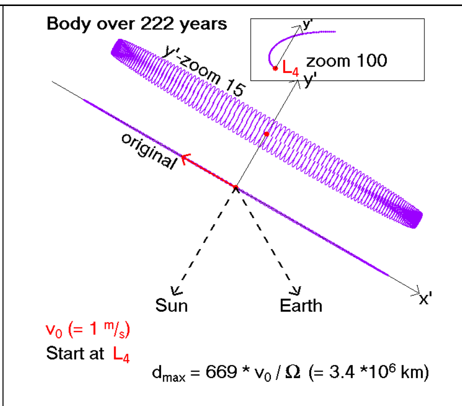

Fig. III.3a

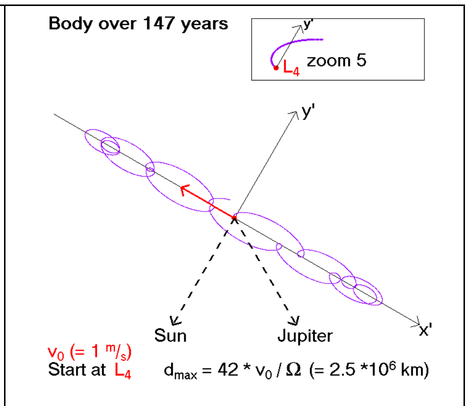

Fig. III.3b

When $\vec{v_0}$ is directed along the y'-axis, d_{max} is considerably smaller because, in the inertial barycenter system, the energy of the body and thus the principal axis of its orbit vary much less.

Jupiter: Roughly 12 ellipse-like loops can be counted, each lasting one Jupiter period.
Earth: The 222 loops cannot be distinguished.
In both cases it is a superposition of an elliptic motion (short period) and a linear oscillation along the x'-axis (long period).

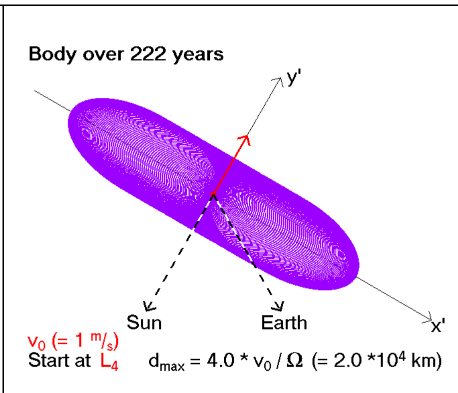

Fig. III.4a

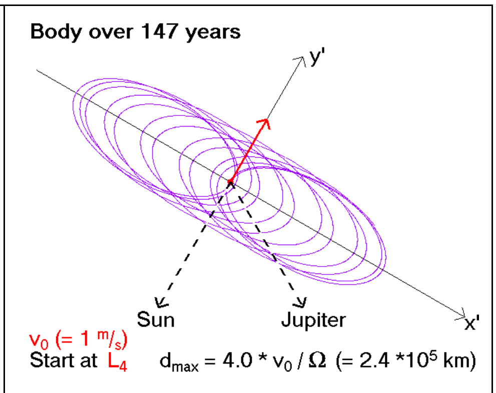

Fig. III.4b

The last examples involve four different planets over a long time of 1000 years: Earth, Jupiter and two even heavier planets replacing Jupiter. The least mass ratio (sun, planet), such that a trojan body can be trapped, is about 24.96. In this sense, the fourth planet almost is the heaviest possible. As the movement of the body is a superposition of periodic oscillations, the body moves within an area with distinct limits.

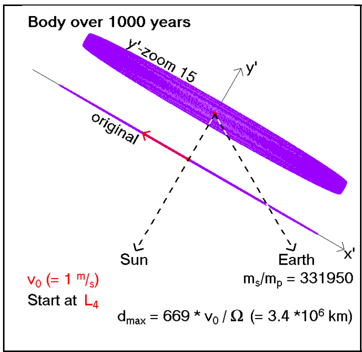

Fig. III.5a

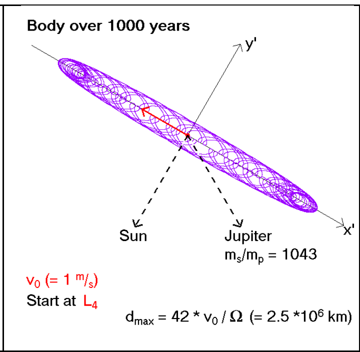

Fig. III.5b

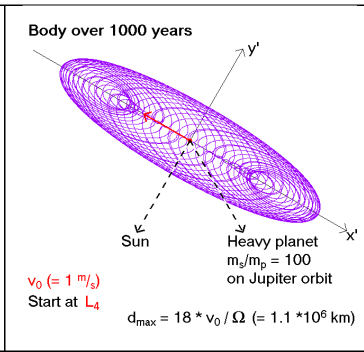

Fig. III.5c

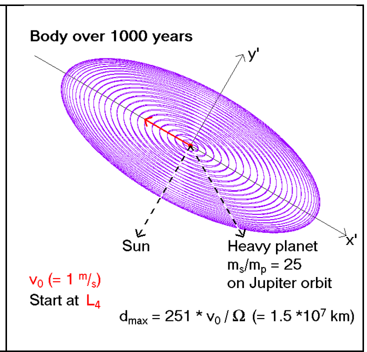

Fig. III.5d

IV Structure of trajectories

The structure is revealed by transforming (2.10) from the (x, y)-system to the (x', y')-system (rotation by 30°) and then using a taylor approximation.

Rotation:

The starting vector $\vec{q} = (x_0, y_0, \dot{x}_0/\Omega, \dot{y}_0/\Omega)^T$ is transformed to

$$\vec{q}\,' = (x_0{}', y_0{}', u_0{}', v_0{}'/\Omega)^T \text{ with } u_0{}' = \dot{x}_0{}'/\Omega \text{ and } v_0{}' = \dot{y}_0{}'/\Omega \qquad (3.1)$$

with $$\begin{pmatrix} x_0{}' \\ y_0{}' \end{pmatrix} = R \begin{pmatrix} x_0 \\ y_0 \end{pmatrix} \text{ and } \begin{pmatrix} \dot{x}_0{}' \\ \dot{y}_0{}' \end{pmatrix} = R \begin{pmatrix} \dot{x}_0 \\ \dot{y}_0 \end{pmatrix}, \quad R = ½ \begin{pmatrix} \sqrt{3} & 1 \\ -1 & \sqrt{3} \end{pmatrix} \qquad (3.2)$$

The matrix of coefficients in (2.10)

$$M_c = \begin{pmatrix} c_1\alpha & c_2\alpha & c_3\beta & c_4\beta \\ 8fc_2 - \gamma c_1 & -(8fc_1 + \gamma c_2) & 8gc_4 - \gamma c_3 & -(8gc_3 + \gamma c_4) \end{pmatrix} \qquad (3.4)$$

is transformed to $M_c{}' = R^{-1} M_c$.

Taylor approximation:

All parameters $g = \sqrt{1-f^2}$, $\alpha = 9 + 4f^2,\ \beta = 13 - 4f^2,\ z = 4(144-\gamma^2)(1-2f^2)$

and $\gamma = \sqrt{27 - 16f^2(1-f^2)}$ (inversion of (2.3))

depend on f only and so does $M_c{}'$.

As $f \leq f_{Jupiter} = 0.0806 \ll 1$, a taylor series of $f \cdot M_c{}'$ makes sense.

The multiplication by f is necessary because $c_2 \sim f^{-1}$ in (2.8). The result is

$$M_c' = \begin{pmatrix} b_1 & 3f^{-1} \cdot a_1 + f \cdot a_3 & -2a_2 & 2b_2 \\ 2a_1 & f \cdot b_3 & b_2 & a_2 \end{pmatrix} + O(f^2) \tag{3.5}$$

with

$$\begin{gathered} a_1 = (0,2,-1,0) \cdot \vec{q}',\ b_1 = (1,0,0,2) \cdot \vec{q}',\ a_2 = (0,0,0,1) \cdot \vec{q}',\ b_2 = (0,-3,2,0) \cdot \vec{q}' \\ a_3 = \tfrac{1}{9}\left(-2\sqrt{3}, 102, -60, -\sqrt{3}\right) \cdot \vec{q}', \quad b_3 = \tfrac{1}{9}\left(-6, 2\sqrt{3}, -\sqrt{3}, -12\right) \cdot \vec{q}' \end{gathered} \tag{3.6}$$

This leads to $\binom{x'}{y'} = \binom{x_1{}'}{y_1{}'} + \binom{x_2{}'}{y_2{}'} + \binom{x_3{}'}{y_3{}'} + \binom{x_4{}'}{y_4{}'} + O(f^2)$ with

$$\begin{aligned} &(1)\ \binom{x_1{}'}{y_1{}'} = 3f^{-1}\binom{a_1}{0}\sin(f\Omega t) && (2)\ \binom{x_2{}'}{y_2{}'} = \binom{b_1}{a_1}\cos(f\Omega \mathrm{t}) \\ &(3)\ \binom{x_3{}'}{y_3{}'} = \begin{pmatrix} 2b_2 \sin(g\Omega \mathrm{t}) - 2a_2 \cos(g\Omega \mathrm{t}) \\ a_2 \sin(g\Omega \mathrm{t}) + b_2 \cos(g\Omega \mathrm{t}) \end{pmatrix} && (4)\ \binom{x_4{}'}{y_4{}'} = f\binom{a_3}{b_3}\sin(f\Omega \mathrm{t}) \end{aligned} \tag{3.7}$$

In this approximation, the trajectory is generated by the superposition of three linear oscillations (1), (2) and (4) with a long period $T_1 = \frac{2\pi}{f\Omega}$ and an elliptic motion (3) with $T_2 = \frac{2\pi}{g\Omega}$.

The major axis of the ellipse coincides with the x'-axis (center at L_4) and the axis ratio is 2:1.

It is useful to consider first the case $f \to 0$ (massless planet):

Motion (4) vanishes, (1) and (2) describe a constant motion: $\begin{pmatrix} 3a_1 \cdot \Omega t \\ 0 \end{pmatrix} + \begin{pmatrix} b_1 \\ a_1 \end{pmatrix}$. For $a_1 \neq 0$, the body runs away from L$_4$. Otherwise the position is fixed at (2) or, with motion (3), the trajectory is the ellipse decribed above (shifted by term (2)).

Normal case $f > 0$:

Motion (1) oscillates along the x'-axis. It has a large amplitude $O(f^{-1})$ such that the body is driven (relatively) far away from L$_4$ ($d_{max} \gg |\vec{q}\,'|$, see 3.1), confirmed by the figures III.2-4. When term (1) does not vanish, a difference between the exact trajectory and its approximation is not visible. This even holds if the minor term (4) is omitted.

Motions (2, 3, 4)

For $a_1 = 0$, term (1) vanishes.

Example: start with $y' = 0$ and $u' = \dot{x}' = 0$ (fig. IV.1a, copy of III.1). The exact trajectory slightly differs from its “smoothed” approximation.

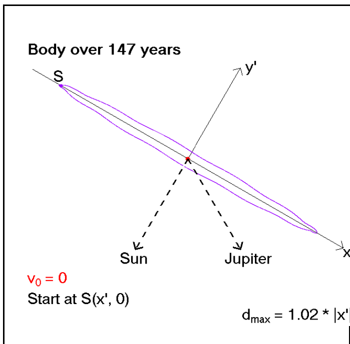

Fig. IV.1a

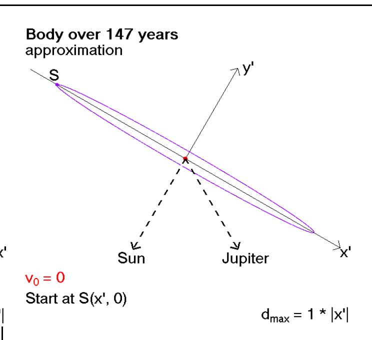

Fig. IV1b

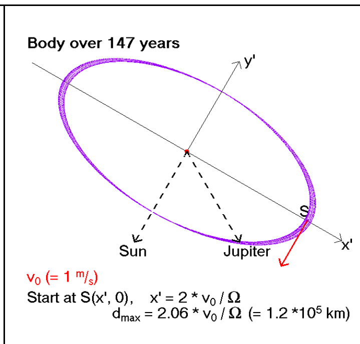

Fig. IV2a

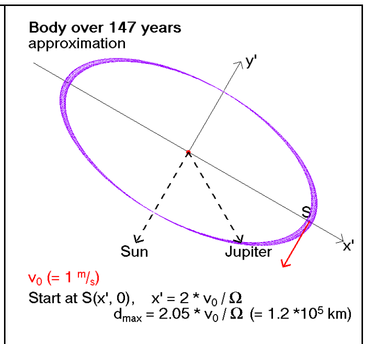

Fig. IV2b

The difference between IV2a and IV2b can only be seen by comparing the values of d_{max}. If term (4) is omitted in this case, a pure ellipse remains. The impact of term (2) is not visible.

V Trajectories leaving the neighborhood of L_4

All figures above are based on the linearized equation of motion, valid for small velocities and distances only. Fig. V.2a is an non-linear extension of fig. III.1b, not only in an algebraic, but also in a geometric sense: The body moves close to a curve and not to a straight line. In fact, S is positioned on the L_4-circle around the barycenter (or the sun, the difference is negligible). The angular distance from L_4 is 10° (90°) in fig.V.2a(b).

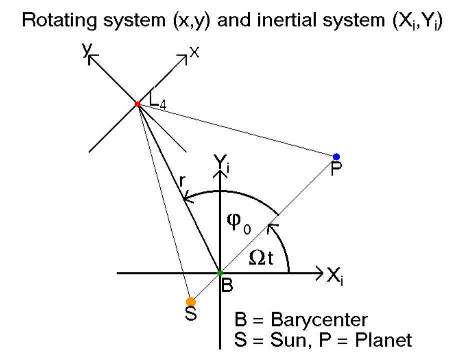

Fig. V.1

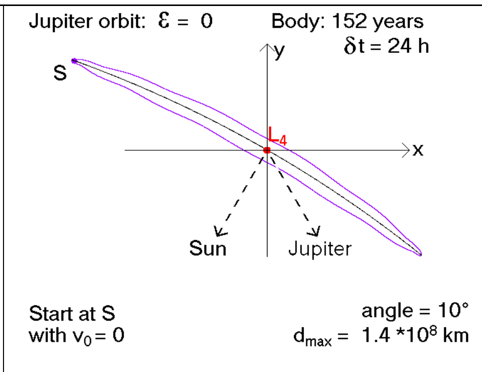

Fig. V.2a

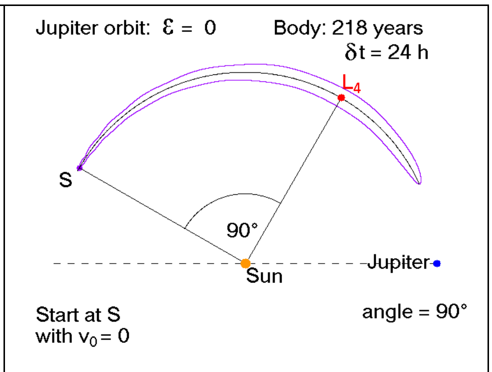

Fig. V.2b

For calculating such extended trajectories, a numeric iteration is needed (chapter X). The execution will be done in the barycenter (X_i, Y_i) − system such that inertial forces do not occur.

Representing the result in the rotating (x, y) −system, (X_i, Y_i) must be rotated back by the angle that L_4 has rotated forward. Tansformation (5.1) is required (fig. V.1):

$$\begin{pmatrix} X_i \\ Y_i \end{pmatrix} = r \begin{pmatrix} \cos(\varphi_0 + \Omega t) \\ \sin(\varphi_0 + \Omega t) \end{pmatrix} + \begin{pmatrix} \cos(\Omega t) & -\sin(\Omega t) \\ \sin(\Omega t) & \cos(\Omega t) \end{pmatrix} \cdot \begin{pmatrix} x \\ y \end{pmatrix}$$

$$\begin{pmatrix} x \\ y \end{pmatrix} = \begin{pmatrix} \cos(\Omega t) & \sin(\Omega t) \\ -\sin(\Omega t) & \cos(\Omega t) \end{pmatrix} \cdot \begin{pmatrix} X_i - r \cdot \cos(\varphi_0 + \Omega t) \\ Y_i - r \cdot sin(\varphi_0 + \Omega t) \end{pmatrix} \tag{5.1}$$

In the case of elliptic planet orbits (next chapter), Ωt must be modified by a slightly different angular function $\varphi(t)$.

The positions of the sun, the planet and the body are updated every 24 hours. In a few cases, the time intervall δt is smaller. It is chosen such that using δt or $\delta t/2$ makes no visible difference.

Fig. V.2a is an extension of IV.4a. The velocity is noted as $\overrightarrow{v_0} = (v_a, v_r)$ where v_a is the azimuthal and v_r the radial velocity.

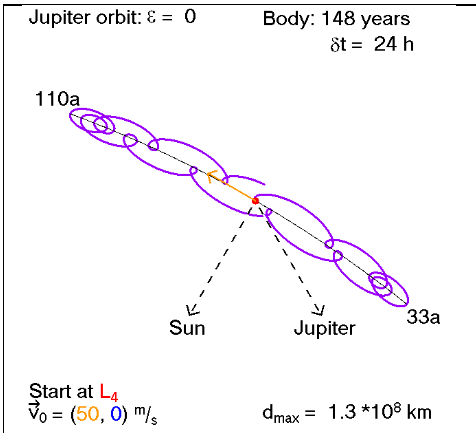

Fig. V.2a

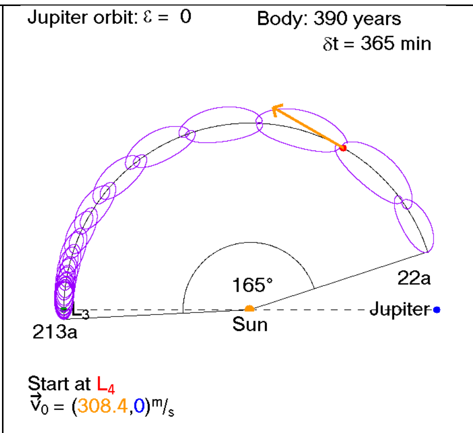

Fig. V.2b

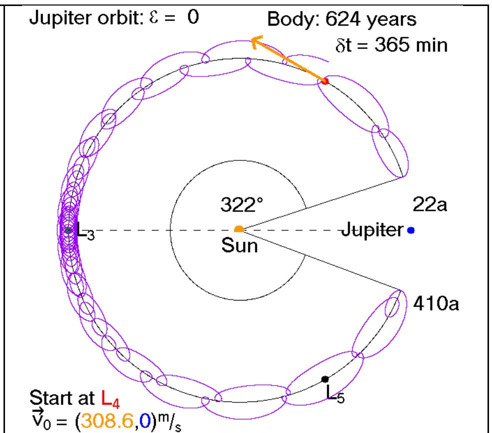

Fig. V.2c

The body starts with different azimuthal velocities at L_4. The greater v_a, the more distinct is the curvature of the trajectory. In V.2b and V.2c the velocities are almost the same, but the trajectories look very different. In both cases, the body moves around the Lagrange point L_3 several times, but then it returns in V.2b whereas, in V.2c, it moves on such that the trajectory is shaped like a horse shoe. By the way, this demonstrates that L_3 is an instable equilibrium point.

The loops around L_3 are more distinct in the adjacent angular diagrams.

Left: Fig. V.2b$_1$
Right: Fig. V.2c$_1$

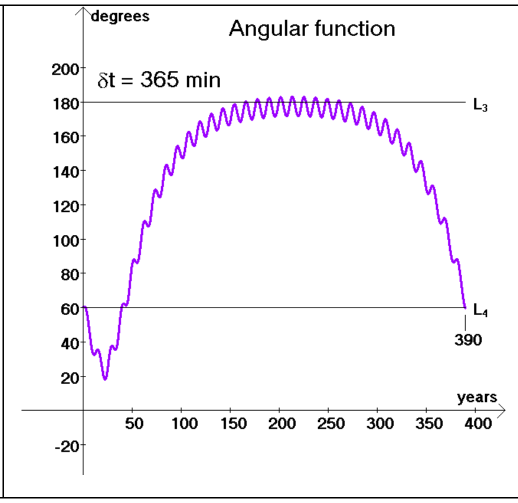

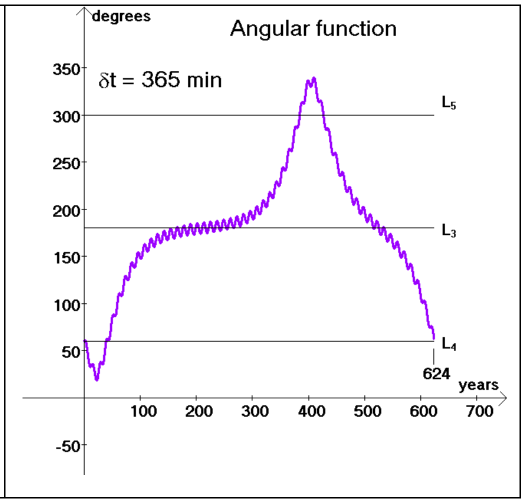

In the corresponding figures of the Sun-Earth system, the radial amplitude is amplified by an r-factor 10 for better visability, corresponding to the y'-zoom in chapter III. The minimum velocitiy for passing L_3 is less than in the case of Jupiter:

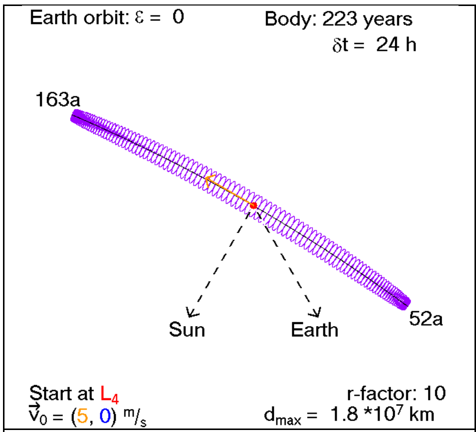

Fig. V.3a

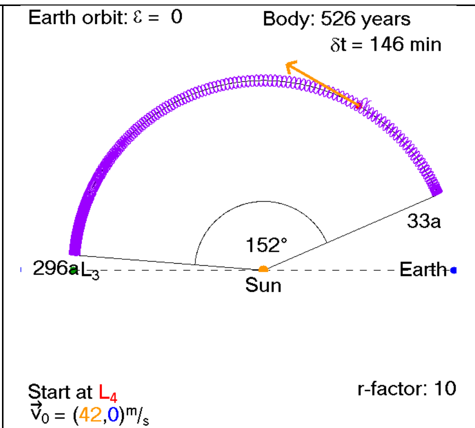

Fig. V.3b

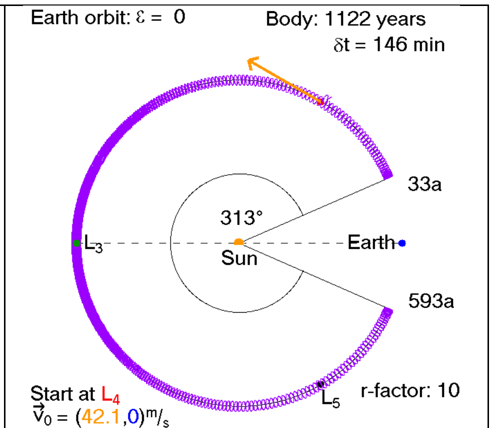

Fig. V.3c

If the starting velocity is purely radial, the angular range depends much less on the velocity.
The figures are extensions of IV.3ab.
Considering the elliptic orbits of Jupiter and Earth (next chapter), the two trajectories are hardly modified.

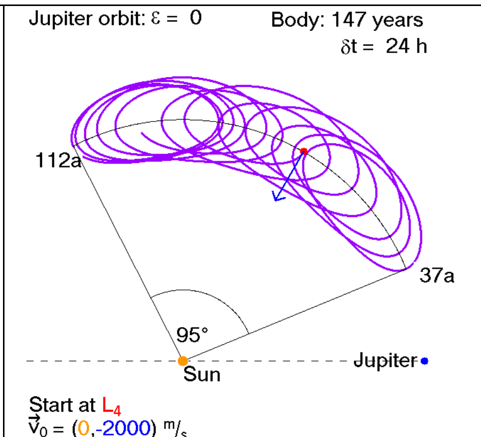

Fig. V.4

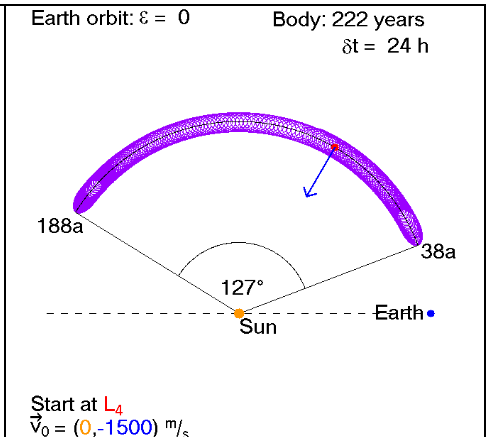

Fig. V.5

VI Trajectories with respect to elliptic planet orbits and perturbations

The orbits of Jupiter ($\varepsilon = 0.0487$) and the earth ($\varepsilon = 0.0167$) are elliptic. In the barycenter system of the sun and the planet, the angular velocity of L_4 (still defined as a vertex of the equilateral triangle Sun-planet-L_4) varies. Nevertheless, L_4 still is an equilibrium point. Therefore, the tajectories do not depend very much on ε ($\ll 1$). See the following figures:

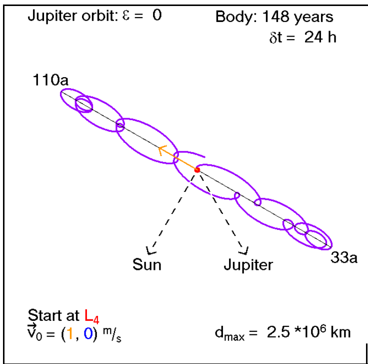

Fig. VI.1a

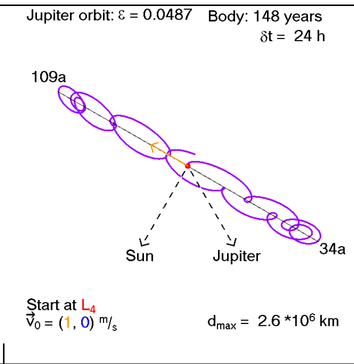

Fig. VI.1b

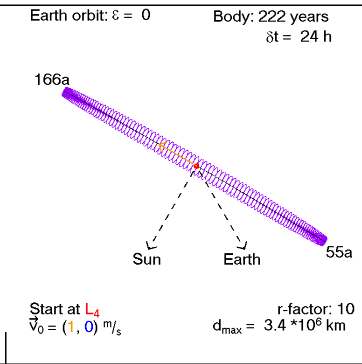

Fig. VI.2a

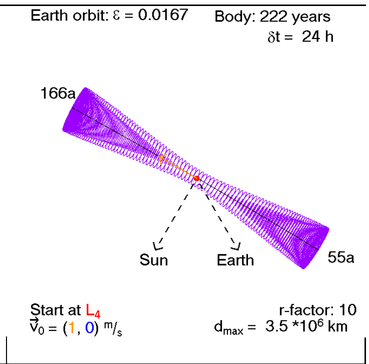

Fig. VI.2b

The values of d_{max} are roughly the same, only the shapes of VI.2a and VI.2b differ near the points of return. However, considering the perturbation by Jupiter, the differences are greater (VI.2c).

In fig. VI.1a - VI.2c, the body starts in L_4 with a moderate azimuthal velocity $v_a = 1m/s$. The excentricity ε and the perturbation by Jupiter do not modify the trajectory very much.

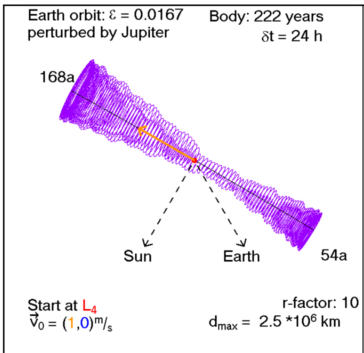

Fig. VI.2c

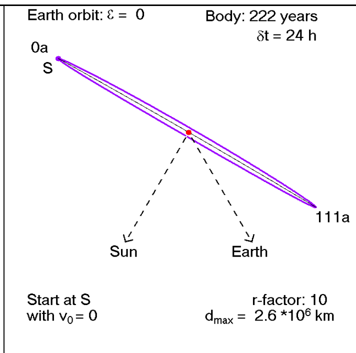

Fig. VI.3a

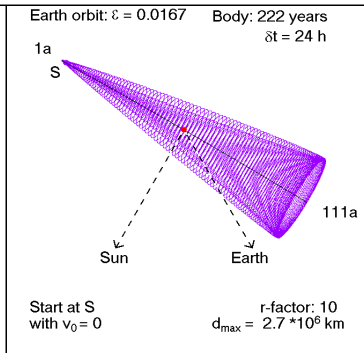

Fig. VI.3b

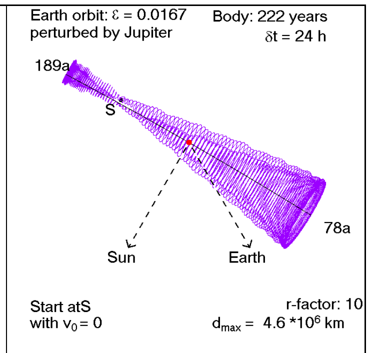

Fig. VI.3c

In VI.3a - VI.3c, the body starts at S ($v_a = v_r = 0$, angular distance from L_4: 1°).

The differences are more distinct. The case S = L_4 is interesting (VI.4ab). Without perturbation, L_4 is an equilibrium point. In VI.4a, the body is very slow (starting with $10^{-8} m/s$) such that $d_{max} = 38\ m$ only. Generally: $v_0 \to 0 \Rightarrow d_{max} \to 0$. This is not true, however, considering the perturbation by Jupiter: $d_{max} \approx 10^6\ km$ for $v_0 = 0$ (VI.4b).

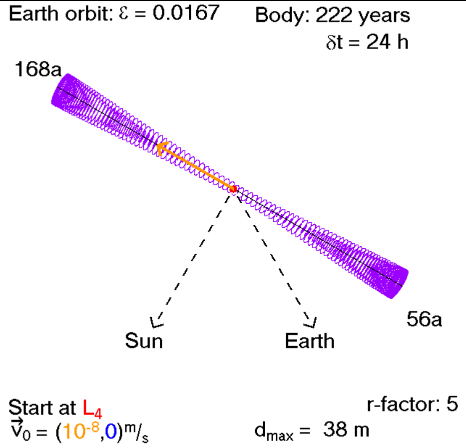

Fig. VI.4a

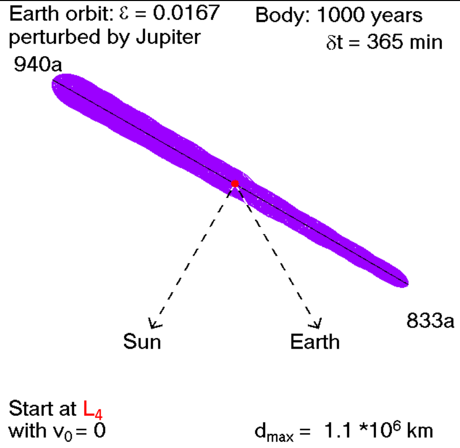

Fig. VI.4b

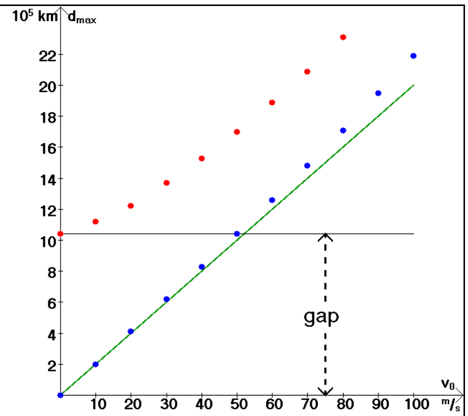

Fig. VI.5

This corresponds to the gap in diagram VI.5 showing d_{max} vs. v_0 with and without perturbation by Jupiter (red and blue dots). The green line shows the deviation from linearity.

VII Trapping a body

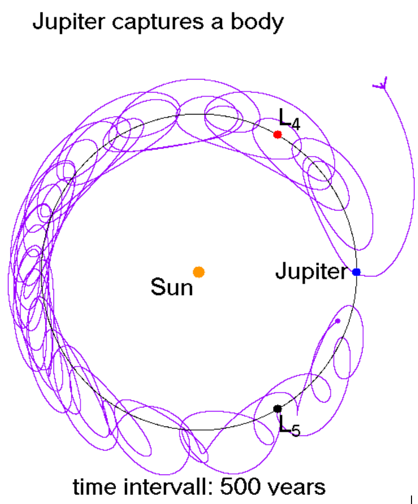

Fig. VII.1

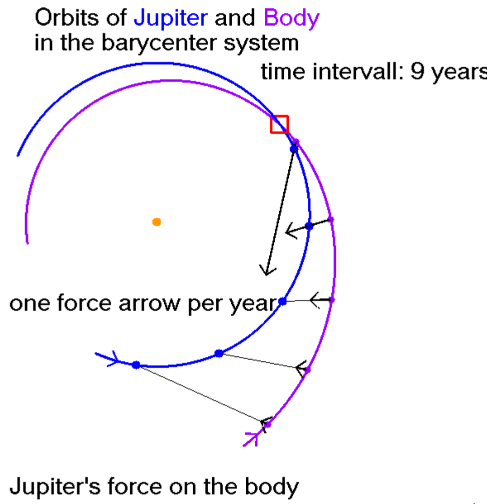

Fig. VII.2

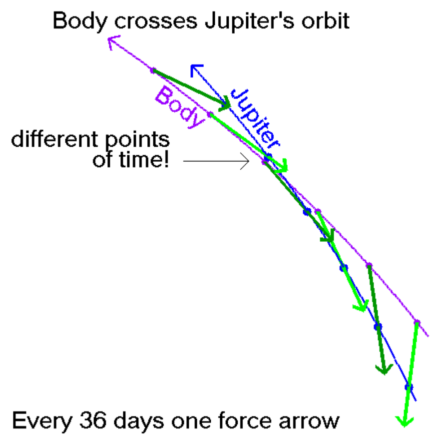

Fig. VII.3

A body approaches Jupiter from far beyond its orbit, slows down by a swing-by effect and then is trapped in a horse shoe trajectory (VII.1). The same process in the non-rotating barycenter system during the first 9 years in VII.2. The slow-down effect essentially takes place in the red square, zoomed in VII.3. Note that the two neighbored points represent different points of time. The reduction of energy in the sun system is shown in VII.4. The initial energy of the body is distinctly negative such that the body was bound to the sun system before. Otherwise it could not have been captured.

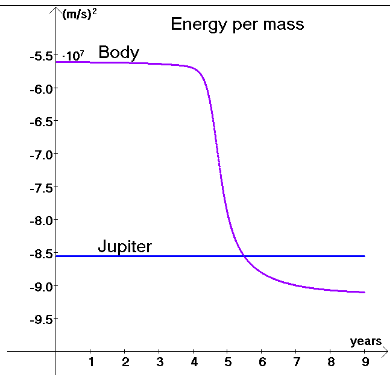

Fig. VII.4

VIII 3D-Extension

The orbit planes of Earth and Jupiter do not differ very much from the ecliptic plane. The orbit of a body, however, may vary much more. If the body does not stay in the neighborhood of L_4, the trajectory typically looks like a horseshoe in the corotating system.

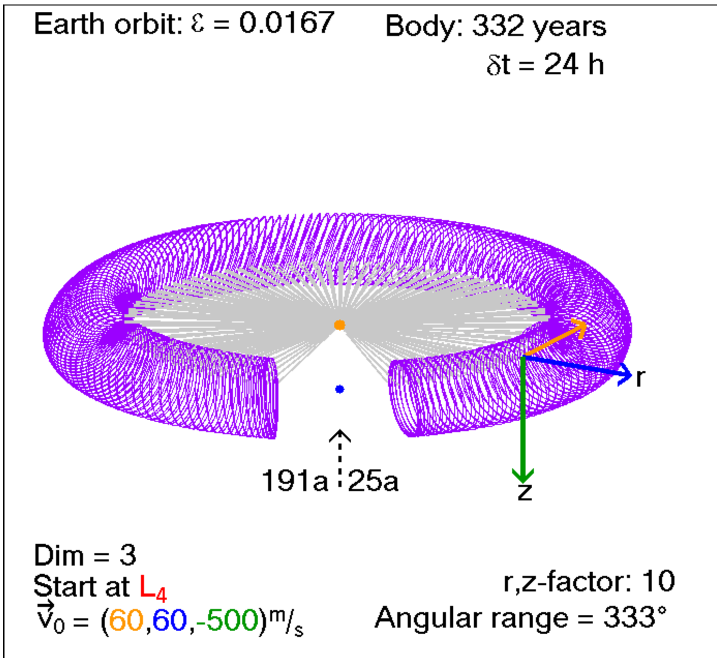

Fig. VIII.1a

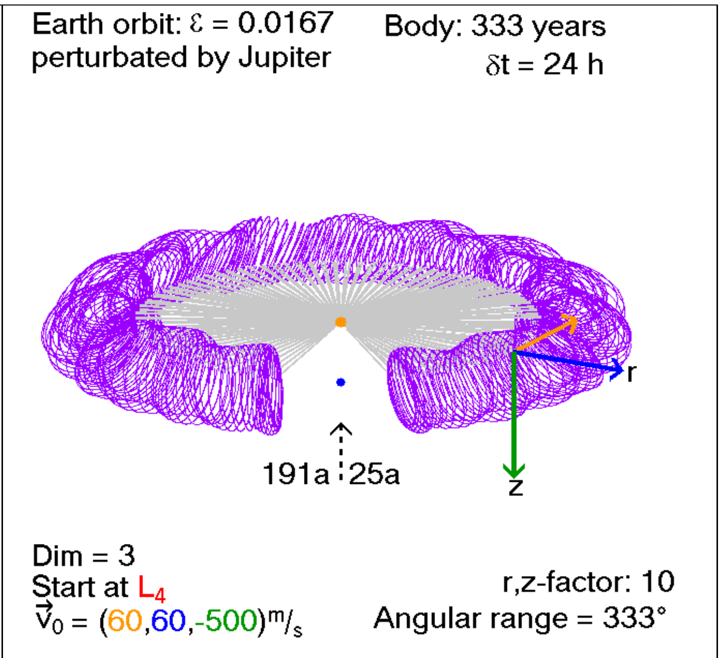

Fig. VIII.1b

Due to the special starting conditions, the trajectory looks more like a torus-shaped spiral (VIII.1a) which is modulated by Jupiter in VIII.1b.

IX Conclusive statements

1. Exact solution of the linearized equation of motion:

a) The trajectory of a body near L_4 essentially is a superposition of four basic (linear or elliptic) oscillations.

b) The maximum distance from L_4 of a body, starting in the neighborhood of L_4 with a velocity $\overrightarrow{v_0}$, depends on its direction. With given $|\overrightarrow{v_0}|$, the body stays the nearer to L_4 the smaller the x'- component is.

2. Extension for a wider range of distances:

Statement 1b) holds if the x'- and y'- components of the velocity are replaced by the azimuthal and radial ones, referring to the L_4-circle.

3. Extension for elliptic planet orbits and perturbations:

a) The modifications for elliptic planet orbits are small as long as the body stays in the neighborhood of L_4.

b) The system Sun-Earth-body is distinctly perturbed by Jupiter for small velocities of the body. A body cannot be trapped closer to L_4 than within a range of about 10^6 km over a long time.

c) This probably holds considering the perturbation caused by all planets because Jupiter's gravity exceeds that of the other planets by far.

X Numeric iteration

The algorithm below is applied to three bodies (Sun, Earth and a massless trojan of the earth) or to four bodies considering the perturbation by Jupiter. The sun can be treated like the other bodies or its motion can be derived from that of the planets by setting the barycenter of the system and its velocity to zero. This way, considering the principle of linear momentum, the approximation error can be reduced.

Details: The position and velocity of each body and the force acting on it is given. This force, depending on the position of all bodies, is updated every time interval δt. Let $\overrightarrow{F_0}$ be the force before such an interval.

a) Assuming a constant velocity, let each body move during the time $p \cdot \delta t, p < 1$.
$\overrightarrow{F_p}$ is the hypothetic force at the new position.

b) Define a time dependent force $\vec{F}(t) = \overrightarrow{F_0} + \left(\overrightarrow{F_p} - \overrightarrow{F_0}\right) \cdot t$

c) By integration, using $\vec{F}(t)$, one finds the approximate position and velocity of each body at the end of the interval δt.

d) The force $\overrightarrow{F_1}$ on each body, measured at the approximate position, differs from $\vec{F}(\delta t)$.
The smaller $\left|\vec{F}(\delta t) - \overrightarrow{F_1}\right|$, the better the approximation. With $p \approx \frac{1}{3}$, the least difference is (heuristically) found. Defining the error $q(\delta t) = \frac{\left|\vec{F}(\delta t) - \overrightarrow{F_1}\right|}{\left|\overrightarrow{F_1}\right|}$, the result is

$$q(24h) < 10^{-5}, q(2.4h) < 10^{-7}.$$

$q(\delta t) \sim \delta t^2$ means a strong tendency to zero.